Optica Applicata, Vol. LIII, No. 1, 2023
DOI: 10.37190/oa230103

Average capacity analysis of FSO system with Airy beam as carrier over exponentiated Weibull channels

YI LI, XINGCHUN CHU, ZHONGXIANG HAN, HANLING TANG, XINKANG SONG

Information and Navigation College, Air Force Engineering University,
Xi'an, Shaanxi 710077, China

Based on scintillation index of Airy beam and exponentiated Weibull channel model, analytical expressions of average channel capacity for free-space optical (FSO) communication links with Airy beam as signal carrier under weak atmospheric turbulence and on-off keying modulation scheme are derived. The average capacity at various propagation distances, transverse scale factors and exponential decay factors has been evaluated. And we compared the average capacity of FSO links with Airy beam and Gaussian beam as signal carrier. The results show that the average capacity of FSO links with Airy beam as carrier increases with the increase of mean signal-to-noise ratio and decreases uniformly with the increase of propagation distance. When the transverse scale factor of Airy beam is about 2 cm, a higher average capacity can be obtained. And the smaller the exponential decay factor of Airy beam, the larger the average capacity. Under the same source power or source width, the average capacity of FSO links with Airy beam as carrier is significantly higher than that of FSO links with Gaussian beam as carrier. The results of this research have some reference significance for the application of Airy beam in FSO communication system.

Keywords: Airy beam, free-space optical communication, channel capacity, exponentiated Weibull model.

1. Introduction

Free-space optical (FSO) communication has become an important direction for the development of space communication technology for its series of advantages in high speed, anti-interference and stealth transmission [1,2]. However, the laser is susceptible to atmospheric turbulence when it propagating in the atmosphere. For the commonly used FSO system with Gaussian beam as signal carrier, scintillation and beam spread caused by atmospheric turbulence are two main factors deteriorating its stability and reliability performance [3,4]. In order to solve these problems, researchers have proposed many methods, such as multi-beam transmission [5], adaptive optics [6], aper-

ture averaging [7], vortex beam [8–10] and modulation encoding in different ways [11]. These methods have reduced the influence of atmospheric turbulence to a certain extent, but the actual suppression effect is not good enough. Therefore, it is a natural idea to replace the traditional Gaussian beam with non-diffracting Airy beam for improving the performance of FSO systems [12].

As a new type of non-diffraction beam, Airy beam has self-accelerating and self -healing properties [13–15]. Compared with the traditional Gaussian beam, Airy beam can keep its transverse intensity distribution constant over a longer transmission distance and has a smaller scintillation index [16,17]. These characteristics enable Airy beams to reduce the effects of diffraction spread and atmospheric turbulence in optical communication and optical design. Therefore, the propagation evolution [18,19], far -field distribution [20], scintillation characteristics [21–23] and beam wander [24] of Airy beam in atmospheric turbulence have been extensively studied. And various applications of Airy beam in optical routing [25], image transmission [26], signal obstacle evasion transmission [27], *etc*., have been reported. However, as far as we know, there are few discussions on the performance of FSO links using Airy beam as optical carrier in the published literature. CHU *et al*. [28] studied the bit error rate (BER) performance of FSO system with Airy beam under the exponetiated Weibull (EW) channel model, and found that the FSO link with Airy beam as carrier has a better average BER performance than the FSO link with Gaussian beam. On this basis, the average channel capacity of FSO links with Airy beam as signal carrier is investigated in this paper under the condition of weak atmospheric turbulence. This research has certain significance for the application of Airy beam to FSO communication field.

The remainder of the paper is organized as follows. In Section 2, the scintillation index expression of Airy beam is deduced. In Section 3, the FSO communication system model and EW channel model with Airy beam as carrier and on-off keying (OOK) modulation are described in detail. Analytical expressions of average channel capacity based on Airy beam, EW fading model and OOK modulation are derived in Section 4. Simulation results are presented and discussed in Section 5. Finally, some conclusions obtained are given.

2. Scintilation index of Airy beam

Turbulence-induced fading is known as scintillation which caused by the random fluctuations of laser intensity and phase due to the non-uniformity of atmospheric refractive index fluctuation. Scintillation is one of the main factors that cause the performance degradation of FSO systems, which can lead to the reduction of channel capacity of communication system. Scintillation index σ_{I}^2 of Airy beam based on first -order Rytov approximation is deduced by EYYUBOĞLU [21].

$$\sigma_{\mathrm{I}}^2 = 0.4147\, k^2 C_n^2 \int_0^L \mathrm{d}p \int_0^{2\pi} \mathrm{d}\varphi_\kappa \int_0^\infty \mathrm{d}\kappa \, \frac{\kappa \exp\left[-\kappa^2 (l_0/5.29)^2\right]}{\left[\kappa^2 + (2\pi/L_0)^2\right]^{11/6}} \times \left\{ \exp\left[-\frac{2(L-p)}{k w_x} a_x \kappa \cos\varphi_\kappa\right] \frac{|\mathrm{Ai}_{x1}|^2 |\mathrm{Ai}_{y1}|^2}{|\mathrm{Ai}_x|^2 |\mathrm{Ai}_y|^2} - \mathrm{Re}\left\{ \exp\left[-\frac{j(L-p)}{k}\kappa^2 \cos^2\varphi_\kappa\right] \frac{\mathrm{Ai}_{x1}\,\mathrm{Ai}_{x2}\,\mathrm{Ai}_{y1}\,\mathrm{Ai}_{y2}}{\mathrm{Ai}_x^2\,\mathrm{Ai}_y^2} \right\} \right\} \tag{1}$$

where

$$\mathrm{Ai}_x = \mathrm{Ai}\left\{ \frac{r_x}{w_x} + \frac{j a_x L}{k w_x^2} - \frac{L^2}{4k^2 w_x^2} \right\} \tag{2}$$

$$\mathrm{Ai}_{x1} = \mathrm{Ai}\left\{ \frac{r_x}{w_x} + \frac{1}{k w_x^2}\left[j a_x L - \kappa w_x (L-p)\cos\varphi_\kappa \right] - \frac{L^2}{4k^2 w_x^2} \right\} \tag{3}$$

and Ai_{x2} is simply Ai_{x1} with sign of k inverted; Ai_y is simply the y equivalent of Eq. (2); Ai_{y1} and Ai_{y2} are the y counterparts of Ai_{x1} and Ai_{x2}, additionally with cosine function changed to sine function. $\mathrm{Ai}(\cdot)$ is the Airy function, w_x, w_y and a_x, a_y are the transverse scale factors and exponential decay factors in X and Y directions respectively, r_x and r_y are the transverse coordinates on receiver plane, L is the propagation distance, κ is the magnitude of spatial wave number and φ_κ indicates its angular orientation, $k = 2\pi n/\lambda$ is the wave number with the wavelength λ, p is the axial propagation distance, C_n^2 is the atmospheric refractive index structure constant, l_0 and L_0 are the inner and outer scales of atmospheric turbulence, respectively.

The scintillation index at the peak position of Airy beam on the receiver plane can be calculated by Eq. (1). While the scintillation index of Gaussian beam has been extensively studied, and the expression can refer to Ref. [29].

3. System and channel model

3.1. System model

On-off keying (OOK) modulation is wildly used in FSO communication systems, which has advantages of simple structure, low cost, and easy implementation [29,30]. It is assumed that the OOK-based FSO communication system has an Airy beam generator and an amplitude modulator. The Airy beam is generated from the Airy beam

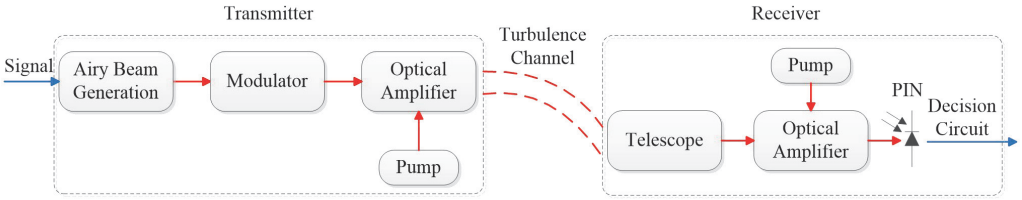

Fig. 1. Block diagram of FSO link for OOK modulation with Airy beam as optical carrier.

generator, then modulated by the modulator, and amplified by the optical amplifier before being emitted. The received optical signal is guided to the optical amplifier, and then the amplified amplitude-modulated optical signal is converted into electrical signal and passed to the decision circuit. Block diagram of FSO communication system for OOK modulation with Airy beam as optical carrier is shown in Fig. 1.

Without considering the influence of atmospheric turbulence, the signal-to-noise ratio (SNR) of a FSO link is defined by

$$\mathrm{SNR}_0 = \frac{i_\mathrm{s}}{\sigma_\mathrm{N}} \tag{4}$$

where i_s is the receiver signal current and σ_N is the root-mean-square noise power.

The mean signal current is represented by

$$\langle i_\mathrm{s} \rangle = \frac{\eta e \langle P_\mathrm{s} \rangle}{h\nu} \tag{5}$$

where $\langle P_\mathrm{s} \rangle$ is the mean signal power in watts, η is the conversion efficiency of the electron/photon detector, e is the electric charge in coulombs, h is Plank's constant (6.63×10^{-34} J·s), and ν is optical frequency in hertz.

The output current variance of the photodetector is defined by

$$\sigma_\mathrm{SN}^2 = \langle i_\mathrm{s}^2 \rangle - \langle i_\mathrm{s} \rangle^2 + \langle i_\mathrm{N}^2 \rangle = \frac{\eta e}{h\nu} \langle \Delta P_\mathrm{s}^2 \rangle + \frac{2\eta e^2 B \langle P_\mathrm{s} \rangle}{h\nu} \tag{6}$$

where $\langle \Delta P_\mathrm{s}^2 \rangle = \langle P_\mathrm{s}^2 \rangle - \langle P_\mathrm{s} \rangle^2$ represents power fluctuations in the signal that become a contributor to the detector shot noise.

Taking atmospheric turbulence and aero-optic into account, the SNR above for a shot-noise limited is defined by the mean SNR [31]

$$\langle \mathrm{SNR} \rangle = \frac{\mathrm{SNR}_0}{\sqrt{\dfrac{P_{\mathrm{s}0}}{\langle P_\mathrm{s} \rangle} + \sigma_\mathrm{I}^2 \mathrm{SNR}_0^2}} \tag{7}$$

where $P_{\mathrm{s}0}$ is the signal power in the absence of atmospheric effects, P_s is the instantaneous input signal power on the photodetector.

The mean SNR can be further expressed as

$$\langle \mathrm{SNR} \rangle = \frac{\mathrm{SNR}_0}{\sqrt{\dfrac{1}{1 + 1.33\,\sigma_\mathrm{R}^2 \Lambda^{5/6}} + \sigma_\mathrm{I}^2 \mathrm{SNR}_0^2}} \tag{8}$$

where $\sigma_\mathrm{R}^2 = 1.23\, C_n^2 k^{7/6} L^{11/6}$ is the Rytov variance, Λ indicates the parameter of dimensionless diffracted beam at the detector. Due to the non-diffraction characteristic of Airy beam within a certain propagation distance, Λ is assumed to 1 for Airy beam analyzed in the following sections.

3.2. EW channel model

Various mathematical models describing the probability density function (PDF) of irradiance fluctuations have been proposed to study the influence of atmospheric turbulence in FSO channel. The most widely accepted distributions are the log-normal (LN) distribution and the gamma-gamma (GG) distribution model. Although these models conform to the actual PDF data in most cases, they are not applicable for all scenarios. The LN model is only suitable for a point receiver in weak turbulence regime. The GG model is considered to be valid for a point receiver in all turbulence regimes, but it does not hold when aperture averaging takes place. The EW distribution model was first proposed by Barrios for the aperture averaging effect under different turbulent regimes. It is suitable throughout the whole weak to strong turbulence regime in the presence of aperture averaging. The PDF of a random variable I described by the EW distribution is given by [32]

$$f(I) = \frac{\alpha\beta}{\eta}\left(\frac{I}{\eta}\right)^{\beta-1} \exp\left[-\left(\frac{I}{\eta}\right)^{\beta}\right]\left\{1 - \exp\left[-\left(\frac{I}{\eta}\right)^{\beta}\right]\right\}^{\alpha-1} \tag{9}$$

where $\alpha > 0$ and $\beta > 0$ are shape parameters related to the scintillation index σ_I^2, $\eta > 0$ is scale parameter related to the mean value of the irradiance. The expressions for shape parameters α, β and scale parameter η are given by [32]

$$\alpha = \frac{7.22\sigma_\mathrm{I}^{2/3}}{\Gamma(2.487\sigma_\mathrm{I}^{1/3} - 0.104)} \tag{10}$$

$$\beta = 1.102(\alpha\sigma_\mathrm{I}^2)^{-13/25} + 0.142 \tag{11}$$

$$\eta = \frac{1}{\alpha\Gamma(1 + 1/\beta)\, g_1(\alpha, \beta)} \tag{12}$$

where $g_n(\alpha, \beta)$ is defined by

$$g_n(\alpha, \beta) = \sum_{i=0}^{\infty} \frac{(-1)^i \Gamma(\alpha)}{i!(i+1)^{1+n/\beta}\Gamma(\alpha-1)} \tag{13}$$

Equation (13) is easily computed numerically for the series converges rapidly [28].

4. Average channel capacity over the EW channel model

Channel capacity is an important metric for estimating the performance of optical communication systems. Considering that channel information can be obtained by the receiver and transmitter of FSO communication system, the average channel capacity of FSO system with OOK modulation is given by

$$\langle C \rangle = \int_0^{\infty} B \log_2(1 + \langle \mathrm{SNR} \rangle I^2) f(I) \mathrm{d}I \tag{14}$$

where B is the channel bandwidth.

With the insertion of Eq. (9) into Eq. (14), we obtain the following expression for the average channel capacity as

$$\langle C \rangle = \int_0^{\infty} B \log_2(1 + \langle \mathrm{SNR} \rangle I^2) \frac{\alpha\beta}{\eta} \left(\frac{I}{\eta}\right)^{\beta-1} \exp\left[-\left(\frac{I}{\eta}\right)^{\beta}\right] \left\{1 - \exp\left[-\left(\frac{I}{\eta}\right)^{\beta}\right]\right\}^{\alpha-1} \mathrm{d}I \tag{15}$$

The $\log(\cdot)$ and $\exp(\cdot)$ functions in Eq. (15) can be represented in terms of Meijer's G function as [33]

$$\log_2(1+z) = \frac{1}{\ln 2} G_{2,2}^{1,2}\left(z\Big|_{1,0}^{1,1}\right) \tag{16}$$

$$\exp(z) = G_{0,1}^{1,0}\left(-z\Big|_{0}^{-}\right) \tag{17}$$

The last term in Eq. (15) can be expanded using Newton's generalized binomial theorem as

$$\left\{1 - \exp\left[-\left(\frac{I}{\eta}\right)^{\beta}\right]\right\}^{\alpha-1} = \sum_{i=0}^{\infty} \frac{(-1)^j \Gamma(\alpha)}{j!\,\Gamma(\alpha-j)} \exp\left[-j\left(\frac{I}{\eta}\right)^{\beta}\right] \tag{18}$$

Combining Eqs. (15)–(18), the average channel capacity represented by Meijer's function can be written as

$$\langle C \rangle = \frac{B}{\ln 2} \frac{\alpha\beta}{\eta} \sum_{j=0}^{\infty} \frac{(-1)^j \Gamma(\alpha)}{j!\,\Gamma(\alpha - j)} \int_0^{\infty} \left(\frac{I}{\eta}\right)^{\beta - 1} G_{2,2}^{1,2}\left(\langle \mathrm{SNR} \rangle I^2 \Big|_{1,0}^{1,1}\right) \times G_{0,1}^{1,0}\left((1+j)\left(\frac{I}{\eta}\right)^{\beta} \Big|_{0}^{-}\right) \mathrm{d}I \tag{19}$$

Equation (19) can be simplified by making the transformation of variables $y = (I/\eta)^2$ and using operational properties of Meijer's G function. The analytical expression of average capacity can be obtained as:

$$\langle C \rangle = \frac{B\alpha\beta}{2\ln 2} \sum_{j=0}^{\infty} \frac{(-1)^j \Gamma(\alpha)}{j!\,\Gamma(\alpha - j)} \frac{\sqrt{k}}{l(2\pi)^{l + (k-3)/2}} \sigma^{-\beta/2} \times G_{2l,\,k+2l}^{k+2l,\,l}\left[\left(\frac{1+j}{k}\right)^k \sigma^{-l} \Big|_{(k,\,0),\,\Delta(l,\,-\beta/2),\,\Delta(l,\,1-\beta/2)}^{\Delta(l,\,-\beta/2),\,\Delta(l,\,1-\beta/2)}\right] \tag{20}$$

where $\sigma = \langle \mathrm{SNR} \rangle \eta^2$, $\Delta(K, A) = A/K, (A+1)/K, ..., (A+K-1)/K$, l and k are positive integer that should meet $l/k = \beta/2$. Equation (20) is given in terms of an infinite series but converges rapidly, and usually about 30 terms or less are sufficient for the series to converge.

5. Numerical results and discussion

5.1. Average channel capacity of FSO link with Airy beam as carrier

In this section, the average channel capacity of FSO link with Airy beam as carrier is numerically evaluated and compared with that of FSO link with Gaussian beam as carrier. In the following simulation, optical wavelength, structure constant, inner and outer scales of turbulence are set as $\lambda = 1550$ nm, $C_n^2 = 10^{-15}$ m$^{2/3}$, $l_0 \to 0$, $L_0 \to \infty$. And x, y symmetry is assumed, so only the x parameter settings are explained. In addition, the setting of receiver plane position is consistent with the peak position of Airy beam at specific propagation distances, because Airy beam experiences propagation distance and source parameters dependent bending [21].

Figure 2 shows the average channel capacity *versus* the mean SNR at different propagation distances. The parameters are selected as $w_x = 2$ cm and $a_x = 0.5$. From Fig. 2, one can see that the average capacity increases with the increase of the mean SNR, and decreases with the increase of the propagation distance. When the mean SNR is less than 5 dB, the effects of propagation distance on the average channel capacity is very small. With the increase of mean SNR, the influence of propagation distance on the average channel capacity becomes more and more obvious, and the average capacity changes uniformly with the change of propagation distance. For example, when the mean SNR is 14 dB, the average channel capacity at propagation distance $L = 1000$,

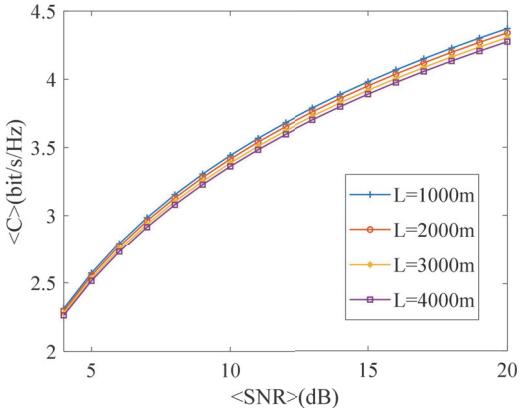

Fig. 2. Average channel capacity *versus* mean SNR for different propagation distances at $w_x = 2$ cm and $a_x = 0.5$.

2000, 3000 and 4000 m are 3.888, 3.858, 3.826 and 3.798 bit/s/Hz, respectively. And the channel capacity decreases about 0.03 bit/s/Hz for every 1000 m increase in propagation distance. When the mean SNR increases to 20 dB, the average channel capacity at above propagation distances are 4.372, 4.341, 4.306 and 4.276 bit/s/Hz, respectively. The channel capacity decreases about 0.032 bit/s/Hz for every 1000 m increase in propagation distance.

The average channel capacity *versus* the mean SNR for selected transverse scale factors at $L = 4000$ m and $a_x = 0.5$ is shown in Fig. 3. As seen from Fig. 3, the influence of transverse scale factor on the average channel capacity increases with the increase of mean SNR. The average channel capacity takes its maximum value at $w_x = 2$ cm and minimum value at $w_x = 3$ cm. Additionally, it increases with the increase of transverse scale factor when $w_x \leq 2$ cm. For example, when the mean SNR is set to 20 dB, the average channel capacity are about 4.295, 4.305, 4.329, 4.347 and 4.275 bit/s/Hz

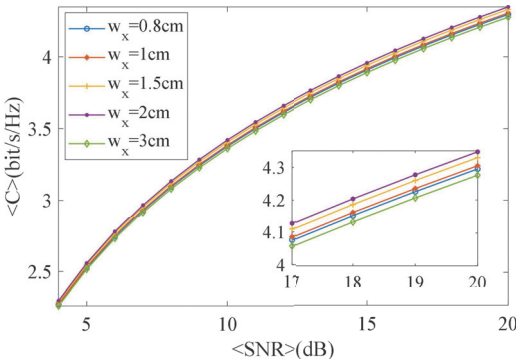

Fig. 3. Average channel capacity *versus* mean SNR for different transverse scale factors at $L = 4000$ m and $a_x = 0.5$.

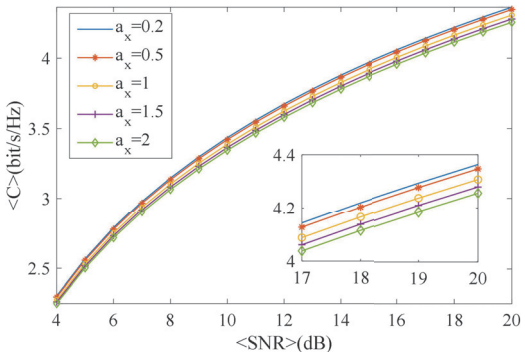

Fig. 4. Average channel capacity *versus* mean SNR for different exponential decay factors at L = 4000 m and w_x = 2 cm.

at transverse scale factor of 0.8, 1, 1.5, 2 and 3 cm, respectively. Therefore, when the transverse scale factor is 2 cm, FSO link with Airy beam as carrier can obtain a higher average channel capacity.

The average channel capacity as a function of the mean SNR at different exponential decay factors is plotted in Fig. 4. The calculation parameters are w_x = 2 cm and L = 4000 m. One can see that the average channel capacity decreases with the increase of exponential decay factor a_x, and the influence of a_x on the average capacity increases with the increase of the average SNR. For example, when the mean SNR is 20 dB, the average capacity are about 4.366, 4.347, 4.307, 4.279 and 4.267 bit/s/Hz at exponential decay factor of 0.8, 1, 1.5 and 2, respectively. This is because the smaller the exponential decay factor of Airy beam, the greater the number of side lobes, and the farther it can propagation without diffraction.

5.2. Comparison of average capacity of FSO links with Airy and Gaussian beams as carrier

In order to compare the average channel capacity of FSO links with Airy and Gaussian beams as carrier, the source power of Airy beam can be calculated by [13]

$$P_{\mathrm{AS}} = \int_{-\infty}^{\infty} \mathrm{Ai}^2\left(\frac{s_x}{w_x}\right) \exp\left(\frac{2a_x s_x}{w_x}\right) \mathrm{d}s_x = \frac{w_x}{\sqrt{8\pi a_x}} \exp\left(\frac{2a_x^3}{3}\right) \tag{21}$$

While the source power of Gaussian beam with waist radius ω_x can be expressed as [21]

$$P_{\mathrm{GS}} = \int_{-\infty}^{\infty} \exp\left(-\frac{s_x^2}{\omega_x^2}\right) \mathrm{d}s_x = \sqrt{\pi}\,\omega_x \tag{22}$$

Firstly, for the case that source power of Airy and Gaussian beams are the same, Eqs. (21) and (22) are equal, and we can obtain

$$\omega_x = \frac{1}{\sqrt{\pi}} P_{\mathrm{AS}} = \frac{w_x}{2\pi\sqrt{2a_x}} \exp\left(\frac{2a_x^3}{3}\right) \tag{23}$$

Therefore, when the source parameters (the exponential decay factor a_x and transverse scale factor w_x) of Airy beam are given, the source parameter (the waist radius ω_x) of Gaussian beam with same power can be calculated, and then its scintillation index can be calculated according to the existing theory.

The average channel capacity of FSO links with Airy and Gaussian beams as carrier *versus* mean SNR under the same source power is shown in Fig. 5. We fix the propagation distance $L = 4000$ m, the exponential decay factor $a_x = 0.5$ and take the transverse scale factor w_x with different values, then the waist radius ω_x of equal-power Gaussian beam is calculated by Eq. (23). As can be seen from the figure, the average capacity of Airy beam link varies obviously with transverse scale factor within the given range of transverse scale factor, while that of equal-power Gaussian beam link is basically unchanged. The average channel capacity of Airy beam link is significantly larger than that of equal-power Gaussian beam link, and the capacity increment of Airy beam link relative to equal-power Gaussian beam link increases with the increase of mean SNR. For example, taking the transverse scale factor as 2 cm, when $\langle \mathrm{SNR} \rangle = 4$ dB, the average capacity of equal-power Gaussian beam link is 1.907 bit/s/Hz, and that of Airy beam link has increased by 0.391 bit/s/Hz, about 2.298 bit/s/Hz. When $\langle \mathrm{SNR} \rangle = 18$ dB, the average capacity of equal-power Gaussian beam link is 3.395 bit/s/Hz, and that of Airy beam link is about 4.204 bit/s/Hz. The capacity increment is 0.809 bit/s/Hz, which is 2 times that at $\langle \mathrm{SNR} \rangle = 4$ dB.

Secondly, we consider the case that the transverse scale factor w_x of Airy beam is the same as the waist radius ω_x of Gaussian beam which can be called source width. Then we can calculate the source power respectively by Eqs. (22) and (23).

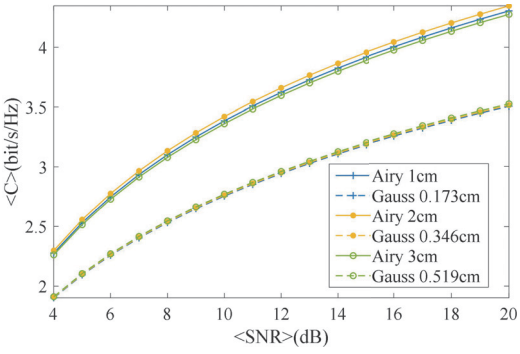

Fig. 5. Comparison of the average channel capacity of FSO links with Airy and Gaussian beam as carrier under the same source power at $L = 4000$ m and $a_x = 0.5$.

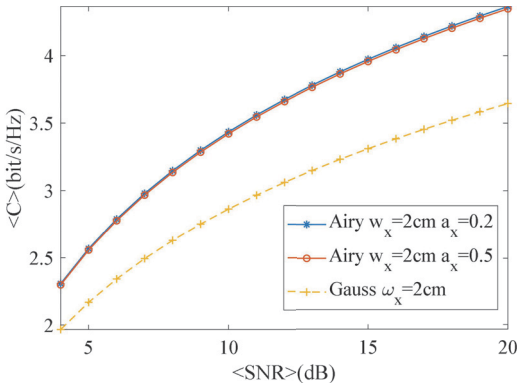

Fig. 6. Comparison of the average channel capacity of FSO links with Airy and Gaussian beam as carrier under the same source width at L = 4000 m and $w_x = \omega_x$ = 2 cm.

In Fig. 6, we fix the source width as 2 cm and plot the average channel capacity of FSO links with Airy and Gaussian beam as carrier *versus* mean SNR. The propagation distance and exponential decay factor is selected to L = 4000 m, a_x = 0.2 and 0.5. It can be seen that the average channel capacity of Airy beam link is still significantly larger than that of Gaussian beam link under the same source width. For example, when $\langle \mathrm{SNR} \rangle$ = 20 dB, the average channel capacity of Gaussian beam link is about 3.645 bit/s/Hz, while that of Airy beam link is about 4.364 and 4.347 bit/s/Hz at a_x = 0.2 and 0.5. Comparing the Gaussian beam curves in Figs. 5 and 6, we can find that the average channel capacity of Gaussian beam link increases with the increase of source width.

6. Conclusion

The average channel capacity of FSO link with Airy beam as carrier under weak turbulence was analyzed. Based on scintillation index of Airy beam and EW channel model, the analytical expression of average channel capacity of FSO link with Airy beam as carrier was derived. Then the average capacity of FSO link with Airy beam as carrier was evaluated numerically and compared with that of FSO link with Gaussian beam as carrier. The results show that the average capacity of FSO link with Airy beam as carrier increases with the increase of mean SNR, and decreases uniformly with the increase of propagation distance. When the transverse scale factor of Airy beam is 2 cm, a relatively large average capacity can be achieved. Decreasing the exponential decay factor of Airy beam, a higher average capacity can be obtained. When the source power of Airy and Gaussian beam are the same, the average capacity of Airy beam link is significantly larger than that of equal-power Gaussian beam link, and the increment of Airy beam link relative to the equal-power Gaussian beam link increases with the increase of mean SNR. Under condition of the same source width, the average capacity of Airy beam link is still significantly larger than the corresponding Gaussian beam

link. In summary, FSO link with Airy beam as carrier has a larger average channel capacity than FSO link with Gaussian beam as carrier. The results obtained will be useful for the application of Airy beam in FSO communication system.

Acknowledgements
This work was supported by the Shaanxi Provincial Natural Science Foundation of China (Grant Number 2019JM-176).

Author contributions
All authors contributed to the study conception and design. All authors read and approved the final manuscript.

Disclosures
The authors declare no conflicts of interest.

References

[1] CHAABAN A., MORVAN J., ALOUINI M., *Free-space optical communications: capacity bounds, approximations, and a new sphere-packing perspective*, IEEE Transactions on Communications **64**(3), 2016: 1176–1191, DOI: 10.1109/TCOMM.2016.2524569.

[2] KAUSHAL H., KADDOUM G., *Optical communication in space: Challenges and mitigation techniques*, IEEE Communications Surveys & Tutorials **19**(1), 2016: 57–96, DOI: 10.1109/COMST.2016.2603518.

[3] BOSU R., PRINCE S., *Mitigation of turbulence induced scintillation using concave mirror in reflection-assisted OOK free space optical links*, Optics Communications **432**, 2019: 101–111, DOI: 10.1016/j.optcom.2018.09.061.

[4] KAUR P., JAIN V.K., KAR S., *Effect of atmospheric conditions and aperture averaging on capacity of free space optical links*, Optical and Quantum Electronics **46**, 2014: 1139–1148, DOI: 10.1007/s11082-013-9845-3.

[5] PELEG A., MOLONEY J.V., *Scintillation reduction by use of multiple Gaussian laser beams with different wavelengths*, IEEE Photonics Technology Letters **19**(12), 2007: 883–889, DOI: 10.1109/LPT.2007.897559.

[6] LI J.W., CHEN W.B., *Bandwidth of adaptive optics system in satellite-ground coherent laser communication*, Chinese Journal of Lasers **43**(8), 2016, 0806003, DOI: 10.3788/cjl201643.0806003.

[7] ANDREWS L.C., *Aperture-averaging factor for optical scintillations of plane and spherical waves in the atmosphere*, Journal of the Optical Society of America A **9**(4), 1992: 97–600, DOI: 10.1364/JOSAA.9.000597.

[8] WANG J., ZHU S.J., WANG H.Y., CAI Y.J., LI Z.H., *Second-order statistics of a radially polarized cosine-Gaussian correlated Schell-model beam in anisotropic turbulence*, Optics Express **24**(11), 2016: 11626–11639, DOI: 10.1364/OE.24.011626.

[9] WANG J., WANG, H.Y., ZHU S.J., LI Z.H., *Second-order moments of a twisted Gaussian Schell-model beam in anisotropic turbulence*, Journal of the Optical Society of America A **35**(7), 2018: 1173–1179, DOI: 10.1364/JOSAA.35.001173.

[10] YANG S., WANG J., GUO M.J., QIN Z.X., LI J.H., *Propagation properties of Gaussian vortex beams through the gradient-index medium*, Optics Communications **465**, 2020, article 125559, DOI: 10.1016/j.optcom.2020.125559.

[11] ZHANG H.G., TANG X., LIN B.J., ZHOU Z.L., LIN C., CHAUDHARY S., GHASSEMLOOY Z., *Performance analysis of FSO system with different modulation schemes over gamma-gamma turbulence channel*, Proc. SPIE 11048, 17th International Conference on Optical Communications and Networks (ICOCN2018), 2019, 1104812, DOI: 10.1117/12.2519711.

[12] CHU X.C., ZHAO S.H., CHENG Z., LI Y.J., LI R.X., FANG Y.W., *Research progress of Airy beam and feasibility analysis for its application in FSO system*, Chinese Science Bulletin **61**(17), 2016: 1963–1974, DOI: 10.1360/N972015-00265.

[13] SIVILOGLOU G.A., CHRISTODOULIDES D.N., *Accelerating finite energy Airy beams*, Optics Letters **32**(8), 2007: 979–981, DOI: 10.1364/OL.32.000979.

[14] SIVILOGLOU G.A., BROKY J., DOGARIU A., CHRISTODOULIDES D.N., *Observation of accelerating Airy beams*, Physical Review Letters **99**(21), 2007, 213901, DOI: 10.1103/PhysRevLett.99.213901.

[15] LIU X., XIA D.N., MONFARED Y.E., LIANG C.H., WANG F., CAI Y.J., MA P.J., *Generation of novel partially coherent truncated Airy beams via Fourier phase processing*, Optics Express **28**(7), 2020: 9777–9785, DOI: 10.1364/OE.390477.

[16] GU Y.L., GBUR G., *Scintillation of Airy beam arrays in atmospheric turbulence*, Optics Letters **35**(20), 2010: 3456–3458, DOI: 10.1364/OL.35.003456.

[17] CHU X.C., ZHAO S.H., FANG Y.W., *Maximum nondiffracting propagation distance of aperture-truncated Airy beams*, Optics Communications **414**, 2018: 5–9, DOI: 10.1016/j.optcom.2018.01.001.

[18] CHEN C.Y., YANG H.M., KAVEHRAD M., ZHOU Z., *Propagation of radial Airy array beams through atmospheric turbulence*, Optics and Lasers in Engineering **52**, 2014: 106–114, DOI: 10.1016/j.optlaseng.2013.07.003.

[19] JI X.L., EYYUBOĞLU H.T., JI G.M., JIA X.H., *Propagation of an Airy beam through the atmosphere*, Optics Express **21**(2), 2013: 2154–2164, DOI: 10.1364/OE.21.002154.

[20] TAO R.M., SI L., MA Y.X., ZHOU P., LIU Z.J., *Average spreading of finite energy Airy beams in non-Kolmogorov turbulence*, Optics and Lasers in Engineering **51**(4), 2013: 488–492, DOI: 10.1016/j.optlaseng.2012.10.014.

[21] EYYUBOĞLU H.T., *Scintillation behavior of Airy beam*, Optics & Laser Technology **47**, 2013: 232–236, DOI: 10.1016/j.optlastec.2012.08.029.

[22] WANG J.A., WANG X.L., GUO L.Y., YING C., PENG Y., *Light intensity scintillation of Airy beam*, Acta Optica Sinica **37**(6), 2017, 0626001, DOI: 10.3788/aos201737.0626001.

[23] LU Q., GAO S.J., SHENG L., WU J.B., QIAO Y.F., *Generation of coherent and incoherent Airy beam arrays and experimental comparisons of their scintillation characteristics in atmospheric turbulence*, Applied Optics **56**(13), 2017: 3750–3757, DOI: 10.1364/AO.56.003750.

[24] WEN W., JING Y., HU M.J., LIU X.L., CAI Y.J., ZOU C.J., LUO M., ZHOU L.W., CHU X.X., *Beam wander of coherent and partially coherent Airy beam arrays in a turbulent atmosphere*, Optics Communications **415**, 2018: 48–55, DOI: 10.1016/j.optcom.2018.01.033.

[25] ROSE P., DIEBEL F., BOGUSLAWSKI, M., DENZ C., *Airy beam induced optical routing*, Applied Physics Letters **102**(10), 2013, 101101, DOI: 10.1063/1.4793668.

[26] LIANG Y., HU Y., SONG D.H., LOU C.B., ZHANG X.Z., CHEN Z.G., XU J.J., *Image signal transmission with Airy beams*, Optics Letters **40**(23), 2015: 5686–5689, DOI: 10.1364/OL.40.005686.

[27] ZHU G.X., WEN Y.H., WU X., CHEN Y.J., LIU J., YU S.Y., *Obstacle evasion in free-space optical communications utilizing Airy beams*, Optics Letters **43**(6), 2018: 1203–1206, DOI: 10.1364/OL.43.001203.

[28] CHU X.C., LIU R.J., LI Y., NI Y.H., WANG X., HAN Z.X., *BER analysis of FSO system with Airy beam as carrier over exponentiated Weibull channel model*, Optical and Quantum Electronics **53**, 2021, 692, DOI: 10.1007/s11082-021-03352-6.

[29] ZHAO J., ZHAO S.H., ZHAO W.H., LI Y.J., LIU Y., LI X., *Average capacity of airborne optical links over exponentiated Weibull atmospheric turbulence channels*, Optical and Quantum Electronics **49**, 2017, 104, DOI: 10.1007/s11082-017-0927-5.

[30] FU Y.L., MA J., YU S.Y., TAN L.Y., *BER performance analysis of coherent SIMO FSO systems over correlated non-Kolmogorov turbulence fading with nonzero boresight pointing errors*, Optics Communications **430**, 2019: 31–38, DOI: 10.1016/j.optcom.2018.08.026.

[31] ZHAO J., ZHAO S.H., ZHAO W.H., LI Y.J., LIU Y., LI X., *Analysis of link performance and robustness of homodyne BPSK for airborne backbone laser communication system*, Optics Communications **359**, 2016: 189–194, DOI: 10.1016/j.optcom.2015.09.082.

[32] BARRIOS R., DIOS F., *Exponentiated Weibull model for the irradiance probability density function of a laser beam propagating through atmospheric turbulence*, Optics & Laser Technology **45**, 2013: 13–20, DOI: 10.1016/j.optlastec.2012.08.004.
[33] KÖLBIG K.S., *Reviews and Descriptions of Tables and Books*, Mathematics of Computation **44**(170), 1985: 573–574.

Received February 22, 2022
in revised form April 19, 2022